Characterization and Modeling of On-Body Spatial Diversity within Indoor Environments at 868 MHz

Simon L. Cotton, *Member, IEEE,* and William G. Scanlon, *Member, IEEE*

***Abstract*—For the first time in the open literature we present a full characterization of the performance of receiver diversity for the on-body channels found in body area networks. The study involved three commonly encountered diversity combining schemes: *selection combination* (SC), *maximal ratio combining* (MRC) and *equal gain combining* (EGC). Measurements were conducted for both *stationary* and *mobile* user scenarios in an *anechoic chamber* and *open office area environment*. Achievable diversity gain for various on-body dual branch diversity receivers, consisting of horizontal and vertical spatially separated antennas, was found to be dependent upon transmitter-receive array separation, user state and level of multipath contribution from the local environment. The maximum diversity gain (6.4 dB) was observed for a horizontal two branch MRC combiner while the transmitter and receiver were on opposite sides of the body, and the user was mobile in the open office area. A novel statistical characterization of the fading experienced in on-body diversity channels is also performed using purposely derived first and second order diversity statistics for combiners operating in Nakagami fading.**

***Index Terms*—Bodyworn channel, diversity, channel characterization, body area network (BAN).**

I. Introduction

CHANNEL conditions for on-body radio links are dictated by a number of different time varying physical and environmental factors. These include: whether the user is stationary or mobile, the relative multipath density of the local surroundings and, most importantly, whether the on-body radio link crosses from one side of the user's body to the other side. Depending on the antenna design and mounting arrangements, there may be additional proximity effects related to antenna-body electromagnetic interaction [1], [2]. Furthermore, although the link distances for on-body applications are relatively short, the systems are often marginal as the transceivers are necessarily compact, low-power devices with limited receiver sensitivity and transmit power, and regulatory limitations may also apply in some applications. Therefore, it is important to fully understand and try to mitigate channel impairments including fading using techniques such as receiver diversity. Here, space, time, frequency or polarization diversity methods may be employed with the aim of providing statistically independent signal versions at the receiver. If the diversity branches are suitably uncorrelated and have comparable mean signal levels, then it is expected that the combination of these signals will have a higher signal-to-noise ratio (SNR) than if one branch is considered in isolation [3].

One method of analyzing on-body propagation effects is to statistically characterize the channel for a chosen scenario, thereby attaching a given probability to the likelihood of a deviation from the mean signal level. A probability density function (pdf) which has recently been used to model channels that incorporate the human body [4]–[7] is the Nakagami-m distribution [8]. It has also been used in the analysis of diversity statistics [9]–[12] for a number of decades. The Nakagami distribution has proven popular due to its ability to approximate the Rice pdf [13] for $m>1$, reduce to the Rayleigh pdf ($m=1$) and describe fading conditions which are worse than Rayleigh ($m<1$). Another important feature of the Nakagami distribution is that it does not place the restriction of uniform magnitude for scattered vectors as observed in the theoretical Rice and Rayleigh fading models. Additionally, analytical second order expressions for diversity reception techniques in Nakagami fading are readily available [14], [15].

A wearable system which will rely upon on-body propagation is the body area network (BAN). There are a number of different IEEE standards in existence which may be used as a basis for BAN communications. One of these is the IEEE 802.15.4 [16] standard which utilizes the 868 MHz (Europe), 915 MHz (US) and 2.45 GHz bands with the aim of providing a low power, low data rate wireless interface between radio devices, hence the focus of this work upon the 868 MHz band. BANs will find use in a number of specialized applications such as patient care where arrays of bodyworn sensors may be configured to form medical networks that can, for example, be used to monitor life vital signs such as body temperature, the heart's electrical activity through electrocardiogram and motor activity. As the requirements of these applications are diverse: indoor and outdoor, fixed and mobile and complex: length of monitoring and amount of transmitted information [17], this presents a significant number of challenges at various layers in the protocol stack. Energy conservation is a particular concern in BAN applications and it is desirable to communicate across the human body reliably with the minimum number of hops and at the lowest possible transmit power levels. The use of spatial diversity in on-body systems could improve operation by reducing the depth and frequency of signal outage, in the process limiting the number of redundant transmissions and increasing battery lifespan. While the possible benefits of bodyworn diversity in applications such as these need to

Manuscript received April 27, 2007; revised October 3, 2007; accepted December 12, 2007. The associate editor coordinating the review of this paper and approving it for publication was G. Durgin.

The authors are with the School of Electronics, Electrical Eng. and Computer Science, Queen's University, Belfast, BT3 9DT, UK (e-mail: {simon.cotton, w.scanlon}@qub.ac.uk).

This work was supported by the UK Department of Employment and Learning and partially funded by the UK Engineering and Physical Science Research Council (EP/D053749/1).

Digital Object Identifier 10.1109/T-WC.2009.070440

be investigated, it is well-known that its implementation will increase complexity and cost per unit, introducing a trade-off between performance and expense.

To the best of the authors' knowledge, we present here for the first time a comprehensive quantitative study of on-body diversity based on experimentation, characterization, modeling and simulation. Significantly, all of the results presented in this paper were obtained with a measurement system based on independent, self-contained, time-synchronized radio receivers that were mounted in close proximity to the human body. Furthermore, as the experimental setup was tetherless, user movement was uninhibited and all potential electromagnetic cable effects were eliminated. We report cross-correlation coefficients between horizontal and vertically separated antennas for a range of on-body channels crossing the upper torso of the human body. The influence of motion and indoor multipath are isolated, and their effect upon on-body diversity characterized. Diversity gain measurements for three combining schemes: selection combination, maximal ratio combining and equal gain combining are also reported in an objective manner. Furthermore, we characterized these channels using diversity-specific first and second order statistics that make provision for the number of signal branches involved, as opposed to non-diversity statistics where the number of branches cannot be accounted for. The associated distribution parameters and theoretical equations are also provided so that our results may be reproduced. A comparison of simulated results using a modified version of the Nakagami waveform simulator proposed in [18] was also performed.

This paper is organized as follows. In Section II, the on-body diversity measurement system, indoor environments and experimental procedure are described. The analysis methods used to process all experimental data, including theoretical first and second order diversity combining statistics in Nakagami fading channels, are presented in Section III. Bodyworn cross-correlation coefficients between spatial branch pairs and diversity gain results are presented in section IV alongside theoretical modeling and simulation of a selection of diversity combined envelopes. In Section V, a brief discussion of possible physical explanations for our observations is presented. Finally some conclusions are drawn in Section VI.

II. Experimental Procedure

A. Bodyworn Antenna Arrays

The on-body diversity measurement system consisted of a portable battery-powered transmitter and two bodyworn arrays, each consisting of four low profile (height, 15.6 mm) helical antennas mounted on its own discrete 25.4 mm diameter groundplane. Each of the antennas were attached to a separate self-contained data logging 868 MHz receiver, allowing the received signal envelope experienced by each element to be recorded and combined later in post-detection analysis. This setup also provided time-synchronization between receivers to ensure a proper diversity analysis was possible, and to facilitate the direct comparison of cross-correlation coefficients, diversity gain, mean signal level and Nakagami first and second order statistics for eight dual diversity combinations over the two arrays. The transmitter used in these experiments was a NovaSource[1] G6 RF synthesized signal source configured to deliver, depending upon on-body transmitter location (Fig.1), either -10 dBm (A & B) or 0 dBm (C & D) of continuous wave through a vertically polarized $\lambda/4$ stub antenna. The receive section of the wearable arrangement was based upon the Crossbow[2] Mica2Dot wireless sensor mote architecture. Each of the units was pre-calibrated and used a modified 3.6 V, 0.95 Ah lithium-thionyl chloride power supply unit. A 10-bit on-board analogue to digital converter was used to quantize the received signal strength indication (RSSI) voltage from the mote's Chipcon[3] CC1000 RF integrated circuit. The receivers were attached in a four-element rectangular array formation to a 3 mm thick, 80% polychloroprene / 20% nylon contoured jacket with sewn on hook and loop mounting pads. The jacket was tight fitting to minimize spurious antenna-body separation effects. As shown in Fig.1, the bodyworn antenna arrays were placed at positions on the user's upper anterior chest region. Array 1 was positioned on the user's right chest and for convenience in notation contained receivers 1 to 4. Likewise, array 2 was situated on the left chest and contained receivers 5 to 8. The transmitter was interchanged between four locations along the perimeter of the waist: front center (A), offset front right (B), offset back right (C) and back center (D), all referenced from the test subject's perspective. The distance from transmitter location to the center of each receive array, as well as the array dimensions in meters are also shown in Fig.1.

B. Indoor Environments

Measurements were taken in an anechoic chamber (54 m^2) and open office area (244.2 m^2) on the ground floor of the ECIT building at Queen's University, Belfast, UK. Fig.2 shows a plan of the measurement environment in relation to the rest of the ground floor. The building was of recent construction, consisting mainly of metal studded dry wall with a metal tiled floor covered with polypropylene-fiber, rubber backed carpet tiles, and a metal ceiling with mineral fiber tiles and recessed louvered luminaries suspended 2.7 m above floor level. The open office area contained a number of soft partitions, PCs, chairs and desks constructed from medium density fiberboard. The anechoic chamber was housed in conductive shielding and lined with pyramidal RF absorbers.

C. Measurement Procedure

The antenna arrays were worn by an adult male of mass 83 kg and height 1.72 m. The transmitter was initially attached to on-body position A at the front center of the user's waist (Fig.1). Both environments were unoccupied for the duration of the measurements. The measurements began with the user stationary in the anechoic chamber at location I (Fig.2) where each data logger was activated to record RSSI voltage at 3.91 ms intervals (256 samples/s). Two consecutive repeated trials with the transmitter at position A were carried out accounting for 7000 (27.3 s) per branch of the total 596000

[1]http://www.nova-eng.com/ (available 08/25/07)
[2]http://www.xbow.com/ (available 08/25/07)
[3]http://www.ti.com/ (available 08/25/07)

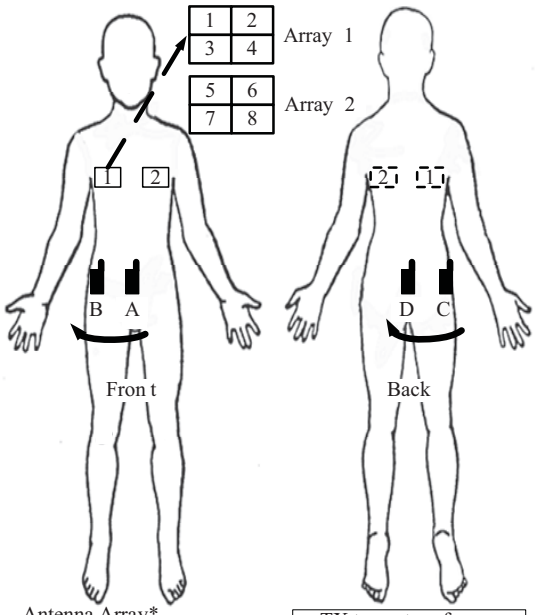

	TX to center of array	
TX Pos	Array 1 (m)	Array 2 (m)
A	0.27	0.28
B	0.25	0.35
C	0.34	0.49
D	0.47	0.50

*Array dimensions in m, antenna = black circle.

Fig. 1. Body diagram showing multiple transmitter locations, receive array positions and dimensions in m. Also shown is the distance from each of the transmitter locations to the center of the respective receive arrays. Array width in wavelengths was 0.25λ, height $= 0.17\lambda$, λ at 868 MHz is 0.345m.

recorded samples for the complete experiment, followed by two mobile measurements (approximate user velocity, 1 ms^{-1}) between I and II. Upon returning to I for the second time, the on-body transmitter was shifted to location B and the process repeated. This procedure was identical for all on-body transmitter locations, for the user both stationary and mobile, in the anechoic chamber and open office area. The stationary measurements in the open office area were carried out at location III and mobile between points III and IV (Fig.2). Thirty-two individual diversity pairs (eight per transmitter location with both horizontal and vertical spatial orientations), were considered for each scenario (user either stationary or mobile) giving a total of 128 diversity combined envelopes over the two environments. The horizontal combinations considered over both arrays were: 1+2, 3+4, 5+6 and 7+8 while vertical spatial separations were restricted to: 1+3, 2+4, 5+7 and 6+8 to permit a manageable analysis of experimental data whilst remaining realistic in terms of potential exploitation.

III. Data Analysis

A. Cross Correlation

Cross-correlation calculations between the signal envelopes for the receiver pairs listed above were performed by concatenating normalized data from each individual trial. Normalization was accomplished by removing the global mean, calculated by averaging the received signal over the entire measurement envelope, from the raw data. For a diversity scheme to be effective, each antenna element should receive

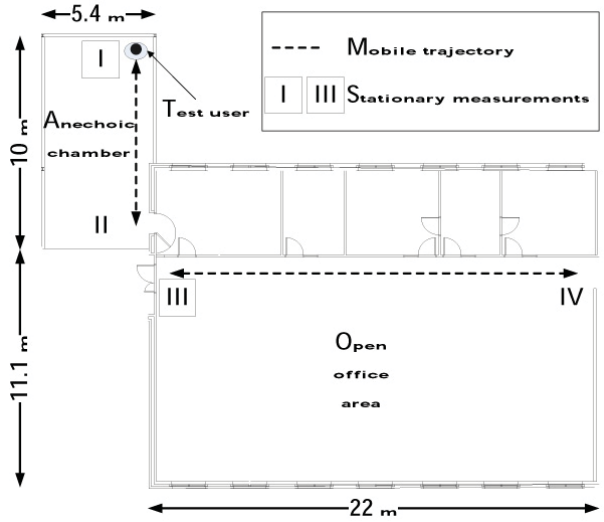

Fig. 2. Plan view of measurement locations showing stationary (I & III) positions and mobile user trajectories (I to II & III to IV).

statistically independent versions of the transmitted signal significantly reducing the likelihood that all branches are experiencing simultaneous fading. As a relative figure of merit [19], two signals are said to be adequately de-correlated if their cross-correlation coefficient (CCC) is less than 0.7. The cross-correlation coefficient, P, of the normalized fast fading envelopes r_1 and r_2 consisting of N samples may be represented by

$$P = \frac{\sum_{i=1}^{N}[r_1(i) - \bar{r}_1][r_2(i) - \bar{r}_2]}{\sqrt{\sum_{i=1}^{N}[r_1(i) - \bar{r}_1]^2}\sqrt{\sum_{i=1}^{N}[r_2(i) - \bar{r}_2]^2}}, \quad (1)$$

where i is the instantaneous sample value, and $\bar{r}_1$ and $\bar{r}_2$ are the respective means of the normalized signal envelopes.

B. Diversity Gain

Three diversity combining techniques were considered: selection, maximal ratio and equal gain combining. SC is a form of switched diversity that provides an output by selecting the branch having the highest input SNR, although often in practice the branch with the largest signal plus noise contribution is used due to the difficulty in measuring SNR [19]. Thus, for a diversity array consisting of M branches, the SC output level R is

$$R = \max(r_1, r_2, \ldots, r_M), \quad (2)$$

where r_M is the signal level observed in the M^{th} branch of the diversity receiver. In postdetection MRC, instantaneous signals in each of the M branches of the receiver are weighted with respect to their squared signal voltage to noise power ratio before being summed. If the local noise power is assumed to be unity for all branches then the output of the two branch maximal ratio combiner given by [20] may be extended to consider M individual receive paths

$$R = \sqrt{(r_1^2 + r_2^2 + \ldots + r_M^2)}. \quad (3)$$

TABLE I
SUMMARY STATISTICS FOR DIVERSITY GAIN AND DIFFERENCE IN MEAN SIGNAL LEVEL (DIMSL) FOR ALL TWO BRANCH SYSTEMS (AC = ANECHOIC CHAMBER, OO = OPEN OFFICE, S = STATIONARY, M = MOBILE, H = HORIZONTAL, V = VERTICAL, MED = MEDIAN)

Environ.	User State	Spatial	SC (dB)			MRC (dB)			EGC (dB)			DIMSL (dB)		
			med	max	min	med	max	min	med	max	min	med	max	min
AC	S	H	0.3	1.5	0.0	2.8	4.0	0.7	2.7	3.9	0.0	2.5	9.0	0.1
		V	0.3	1.9	0.0	2.7	4.2	1.5	2.6	4.1	1.2	2.6	4.8	0.4
	M	H	0.1	1.4	0.0	2.4	3.8	0.1	2.2	3.8	-1.8	2.2	17.5	0.7
		V	0.1	1.4	0.0	2.5	3.8	0.7	2.4	3.7	-0.1	2.6	10.7	0.5
OO	S	H	0.2	3.3	0.0	2.3	5.2	1.7	2.2	4.9	1.5	2.1	4.5	0.4
		V	0.1	2.8	0.0	2.2	4.7	1.3	2.0	4.6	0.6	2.5	4.2	0.1
	M	H	1.4	4.9	0.0	3.3	6.4	1.7	3.2	5.8	0.9	2.5	5.1	0.3
		V	1.4	3.2	0.0	3.3	4.6	1.4	3.0	4.2	0.8	2.3	4.2	0.2

The complexity of producing weighted coefficients in MRC may be reduced by using postdetection EGC where all weighting factors are assumed to be constant. In a similar manner to (3), if it is assumed that the local noise power in all branches is unity, the equation for two branch EGC [21] may be altered to consider M antenna elements

$$R = \frac{(r_1 + r_2 + \ldots + r_M)}{\sqrt{M}}. \tag{4}$$

An important concept in diversity is that of *diversity gain*. Turkmani *et al* [21] give an empirical definition of this as the difference in signal level of the branch with the higher mean and that of the output of the diversity combiner for a given probability or signal reliability. Diversity gain is therefore dependent on the cross-correlation and power imbalance between branches. All diversity gain calculations in this paper are made at a signal reliability of 90% (cumulative probability = 0.1).

C. Diversity Statistics in Nakagami Fading Channels

It was demonstrated in [4] that the fading experienced in on-body channels which traverse the upper torso while the user was stationary or mobile in an indoor environment could be described by Nakagami first and second order statistics. Under the assumption of identical Nakagami fading conditions, equal noise power and independence between diversity branches, closed-form formulae for the cdfs of SC and MRC in the presence of Nakagami distributed fading are presented in [14]. The level crossing rate of the diversity combined envelope may be defined as the number of positive (or negative) transitions beyond a threshold level R in a given amount of time. The LCR (N_R) is expressed analytically in terms of the time derivative $\dot{r}$ of the combined envelope r and the joint probability of $\dot{r}$ and r at $r = R$

$$N_R = \int_0^\infty \dot{r} p(\dot{r}, r = R) d\dot{r}. \tag{5}$$

For a selection combining scheme with M diversity branches operating in Nakagami fading conditions, the LCR (N_R), normalized to the maximum Doppler frequency f_m, may be represented by [14]

$$\frac{N_R}{f_m} = \frac{\sqrt{2\pi} M \Gamma^{M-1}(m, m\rho^2)}{\Gamma^M(m)} (m\rho^2)^{m-0.5} \exp(-m\rho^2), \tag{6}$$

where m is the Nakagami fading parameter, Ω the mean power, and ρ is the normalized threshold level $(R/\sqrt{\Omega})$. $\Gamma(a)$ and $\Gamma(a, b)$ denote the complete and incomplete Gamma functions, respectively. The average fade duration, T_R, of the diversity combined envelope is the total time spent below a threshold level R divided by the number of individual fades and is estimated as

$$T_R = \frac{cdf(r = R)}{N_R}. \tag{7}$$

The normalized Nakagami AFD (T_R) formula for M-branch SC is given by [4]

$$T_R f_m = \frac{\Gamma(m, m\rho^2) \exp(m\rho^2)}{\sqrt{2\pi} M (m\rho^2)^{m-0.5}}. \tag{8}$$

The normalized LCR and AFD statistics for MRC are accordingly listed in equations (9) and (10).

$$\frac{N_R}{f_m} = \frac{\sqrt{2\pi}}{\Gamma(mM)} (m\rho^2)^{mM-0.5} \exp(-m\rho^2). \tag{9}$$

$$T_R f_m = \frac{\Gamma(mM, m\rho^2) \exp(m\rho^2)}{\sqrt{2\pi} (m\rho^2)^{mM-0.5}}. \tag{10}$$

No closed-form expression exists for the solution of the M-branch Nakagami EGC pdf. In [15], for i.i.d. channels the pdf of the EGC envelope r is expressed as

$$p(r) = \sqrt{M} \int_0^{\sqrt{M}r} \int_0^{\sqrt{M}r - r_M} \cdots \int^{\sqrt{M}r - \sum_{i=3}^{M} r_i} \times [p_1(r)(r\sqrt{M} - \sum_{i=2}^{M} r_i) \prod_{i=2}^{M} p_i(r_i)] dr_2 \ldots dr_M. \tag{11}$$

Under the assumption of branch envelopes with identical Nakagami parameters, and by restricting the number of available diversity branches to M = 2, Iskander ([16], equation (38)) reduced equation (11) to

$$p(r) = (\frac{m}{\Omega})^{2m} \frac{2B(2m, \frac{1}{2})}{[\Gamma(m)]^2 2^{2m-2}} r^{4m-1} \exp(-2\frac{m}{\Omega} r^2) \times \Phi(2m, 2m + \frac{1}{2}, \frac{m}{\Omega} r^2), \tag{12}$$

where $B(a, b)$ is the beta function and $\Phi(a, b, c)$ is the confluent hypergeometric function. Following from this, the normalized LCR for dual-branch EGC is given as

$$\frac{N_R}{f_m} = \frac{\sqrt{2\pi} B(2m, \frac{1}{2})}{[\Gamma(m)]^2 2^{2m-2}} (\frac{m}{\Omega} r^2)^{2m-0.5} \exp(-2\frac{m}{\Omega} r^2) \times \Phi(2m, 2m + \frac{1}{2}, \frac{m}{\Omega} r^2). \tag{13}$$

Using the infinite series representation of the cdf for two-branch EGC, equation (40) in [15], allows the normalized AFD to be represented by

$$T_R f_m = \frac{\exp(2\frac{m}{\Omega}r^2)\sum_{n=0}^{\infty}\frac{\Gamma(2m+n)}{\Gamma(2m+n+\frac{1}{2})}\frac{\Gamma(2m+n,2\frac{m}{\Omega}r^2)}{2^n n!}}{2B(2m,\frac{1}{2})(2\frac{m}{\Omega}r^2)^{2m-0.5}\Phi(2m,2m+\frac{1}{2},\frac{m}{\Omega}r^2)}. \quad (14)$$

IV. Results

A. Cross-Correlation Coefficients

As each of the receiver units was an integrated RF device, the mutual coupling ($|S_{21}|$) between antenna array elements was measured using two modified antenna boards and a Rohde & Schwarz ZVB-8 vector network analyzer. The antenna boards were identical to those used in the diversity measurements with the addition of a coaxial connector below the groundplane. When these were mounted with the appropriate antenna-body and element spacing (described in Section II), the mutual coupling was found to be -23.5 dB at 868 MHz. The loading condition, as seen by the antenna at the receiver input port, was also measured for a number of the devices using a purposely developed RF interface board (that replaces the antenna with a coaxial connector) and found to be typically 40 + j15 Ω at 868 MHz. Furthermore, the mutual coupling between elements is also a potential source of RF interference because of unintentional radiation such as local oscillator leakage. Thus, the overall signal to interference ratio for the study was determined by switching off the transmitter and measuring the RSSI voltage at each receiver prior to each session. The lowest recorded signal to interference ratio was 1.4 dB for the transmitter at position D while the user was mobile in the open office area. This confirmed that the measurements were made above the system noise floor as all relevant factors including receiver noise and mutual coupling were taken into account.

The cross-correlation coefficients themselves varied between -0.70 (1+2 of array 1, user stationary, anechoic chamber, transmitter at A) and 0.95 (5+6 of array 2, user mobile, anechoic chamber, transmitter at A). In general, CCCs were found to be greater in anechoic conditions with values for 52 out of a possible 64 horizontal combinations in excess of those obtained in the open office area. Fig.3 shows the cdf of CCCs for all horizontal combiners for all measured scenarios. It is clear that CCCs were normally less than 0.70 when the user was stationary in either environment, or mobile in the open office area. A similar trend was observed for vertical combinations, with 75% of CCCs greater for the anechoic chamber compared to the open-office area and these were also typically less than 0.70. These results indicate that, although the separation between elements is much less than $\lambda/4$ [22] (0.12λ horizontal, 0.09λ vertical), the implementation of either spatial configuration for on-body antenna diversity (assuming comparable mean signal levels) should produce a worthwhile improvement in the overall communications system performance.

B. Diversity Gain and Difference in Mean Signal Level

1) User Stationary: Here, diversity statistics were largely similar for both the reduced multipath conditions of the anechoic chamber (for on-body systems local multipath fading is produced by reflected and scattered waves generated by the body due to respiration and other body movements) and the open office area. At location I, the median value of diversity gain (for all horizontal combinations in both arrays, over all transmitter positions) was found to be 0.3 dB, 2.8 dB and 2.7 dB for SC, MRC and EGC, respectively. The corresponding maxima, diversity gain denoted G with the scheme in subscripts, ($G_{SC} = 1.5$ dB, $G_{MRC} = 4.0$ dB, $G_{EGC} = 3.9$ dB), all occurred for the horizontal combination of branches 7+8 of array 2 with the transmitter at A. However, as the transmitter position was changed from A through to D, the diversity gain tended to decrease with minima of: G_{SC} (0.0 dB), G_{MRC} (0.7 dB) and G_{EGC} (0.0 dB), all occurring for the combination of branches 3+4 of array 1, with the transmitter at D.

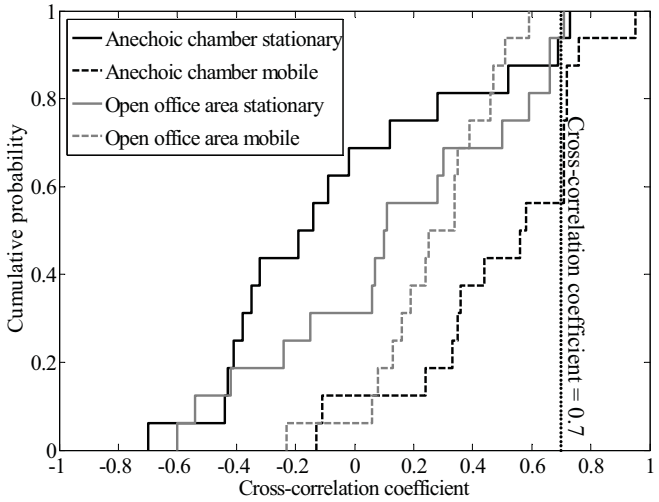

Fig. 3. Cumulative distribution functions of cross-correlation coefficients for horizontally separated on-body antennas.

The effect of varying transmit-receive array separation on diversity statistics was investigated using Pearson's product-moment to calculate the linear correlation. Although it will not detect curvilinear dependencies and its interpretation should be based on practical significance, it is nonetheless a useful estimator in determining whether or not an underlying relationship exists. The linear correlation coefficient (represented by r subscript scheme) between diversity gain and distance to the center of the array was found to be $r_{SC} = -0.53$, $r_{MRC} = -0.65$, and $r_{EGC} = -0.66$. This suggests that, for a stationary user in an anechoic environment, an inverse relationship between on-body distance and diversity gain exists when using horizontal combiners.

In the anechoic chamber, the difference in mean signal level (DIMSL) increased between horizontal branches as the transmitter was moved from front to the back of the body (A to D). Pearson's product-moment was also calculated to assess correlation between diversity gain and DIMSL with coefficients of -0.79, -0.84 and -0.87 for SC, MRC and EGC, respectively. These results confirm the dependence of diversity gain upon comparable mean signal levels between combiner branches. The horizontal space diversity gain results for the open office area were shown to deteriorate much

more rapidly as the transmitter is moved around the user's waist. For example, all horizontal SC combinations for array 1 in the anechoic chamber offered some diversity gain for all transmitter positions except D. However, in the open office area the same set of SC combiners offered no diversity gain for both C and D transmitter positions. Here, evidence for negative correlation between transmitter position and diversity gain was not as strong as that observed in the anechoic chamber ($r_{SC} = -0.31$, $r_{MRC} = -0.53$, $r_{EGC} = -0.56$).

Overall, the diversity gain and DIMSL statistics for vertical combinations were similar to those obtained for horizontal (Table I). However, the same dependency between transmitter location and diversity gain was not observed as the correlation coefficients in the anechoic chamber were 0.11, 0.06 and 0.06 for SC, MRC and EGC, respectively. This was confirmed by visual inspection of data scatter plots and indicates that, in this study, vertically separated bodyworn antennas are less sensitive to transmitter location than horizontal.

2) User Mobile: For all horizontal combiners over both arrays, user movement in the anechoic chamber produced comparable (typically within 0.4 dB) median diversity gain to the stationary case, with a moderate increase in the minimum values for MRC and EGC and maximums of all three schemes (Table I). However, the mobile scenarios exhibited positive correlation between transmitter - receive array separation distance and diversity gain, rather than the negative correlation associated with the stationary measurements. In the anechoic chamber, Pearson's product moment correlation coefficient had an average value of 0.38 but this substantially increased in the open office area ($r_{SC} = 0.79$, $r_{MRC} = 0.71$, $r_{EGC} = 0.65$). Table II shows the diversity gain statistics in detail for the user mobile in the open office area. In general, horizontally combined receivers provided higher diversity gain over vertical ones. The antenna array situated on the left chest (array 2) offered greater diversity gain for both horizontal and vertical separations which is intuitive as the median DIMSL was lower than that for array 1.

In terms of overall diversity gain for the complete experiment, the horizontal combination 7+8 in array 2 performed best while the transmitter was located at position C and the user mobile in the open office area ($G_{SC} = 4.9$ dB, $G_{MRC} = 6.4$ dB, $G_{EGC} = 5.8$ dB, Table II). The DIMSL and CCC for this set of receivers were 1.6 dB and 0.13, respectively. Fig.4(a) shows the complete received power profile and, for illustrative purposes, Fig.4(b) an expanded view of the time series between 10 and 12 s, for 7+8 combined using MRC (traces for SC and EGC have been omitted for clarity). Fig.5 shows the cdf of each of the systems compared to the branch with the highest mean signal level (branch 7). Here, all three diversity schemes eliminate fading at 5 dB below the mean signal level of the branch with the highest average power, for the required signal reliability. More poignantly, if an MRC system architecture was adopted at the receiver the 6.4 dB diversity gain could be translated into a reduction in the required transmitter power by a factor of 4, significantly increasing the lifespan of the portable supply which may be advantageous in niche applications such as medical body area networks.

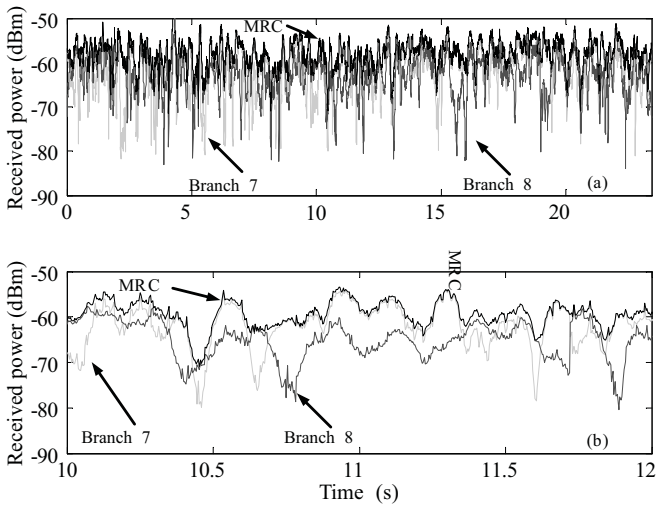

Fig. 4. (a) Received power profile for horizontally spaced branches 7 (light grey) and 8 (medium grey) of array 2 combined using MRC (black) while the user was mobile in the open office area with transmitter at position C, (b) time series expansion between 10 and 12 s.

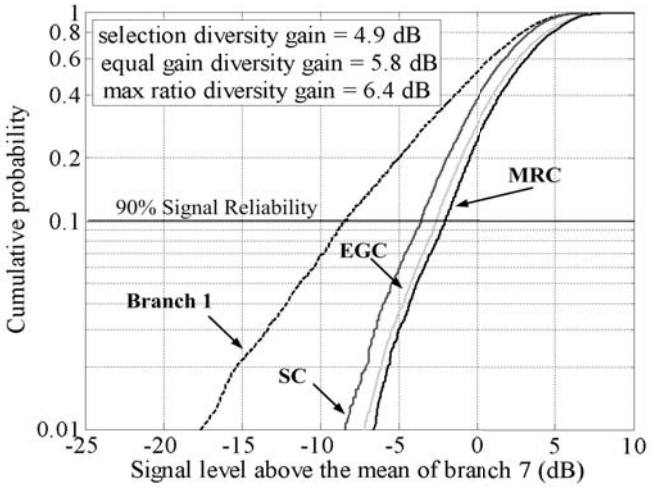

Fig. 5. Cumulative distribution function for two branch (7+8) bodyworn spatial diversity system while the user was mobile in the open office area with transmitter at position C.

C. On-Body Diversity Combining Statistics

1) User Stationary: To enable the fading characteristics observed at the output of the virtual combiners analyzed in this study to be approximately reproduced, we now present a selection of the Nakagami m and Ω parameters obtained from each of the combined signal envelopes, normalized to the global mean. All diversity combining parameter values were estimated on a 95% confidence interval using maximum likelihood (ML) estimation. Due to the complexity of obtaining the derivative of the log-likelihood function for SC and EGC, a constrained quasi-Newton approach using the fmincon(·) optimization algorithm available in Matlab was used to minimize the negative log-likelihood function (equivalent to maximizing the log-likelihood) over the bounded parameter space Θ. It should be noted, unless otherwise specified, that all Nakagami-m and Ω parameters presented in this section refer to the case when there are two available signal branches (i.e.,

TABLE II
DIVERSITY GAIN AND DIMSL (IN DECIBELS) FOR ALL TWO BRANCH SYSTEMS FOR A MOBILE USER IN THE OPEN OFFICE AREA ENVIRONMENT

Transmitter Position	Horizontal					Vertical				
	Branches	SC	MRC	EGC	DIMSL	Branches	SC	MRC	EGC	DIMSL
A	1+2	0.1	2.1	1.9	2.8	1+3	0.0	1.8	1.6	2.2
	3+4	0.0	1.9	1.7	2.5	2+4	0.2	2.1	2.0	2.4
	5+6	0.2	2.0	1.9	2.5	5+7	2.0	4.2	4.1	0.7
	7+8	1.2	3.3	3.2	0.3	6+8	0.0	1.6	1.3	3.4
B	1+2	1.2	3.3	3.2	1.7	1+3	1.1	3.2	3.1	3.7
	3+4	1.5	3.6	3.4	2.9	2+4	0.4	2.6	2.4	2.5
	5+6	0.5	2.6	2.4	1.9	5+7	0.1	2.0	1.8	2.5
	7+8	0.5	2.4	2.2	2.1	6+8	0.4	2.5	2.4	1.5
C	1+2	3.1	4.6	4.1	3.1	1+3	0.2	1.4	0.8	2.7
	3+4	0.6	1.7	0.9	5.1	2+4	1.7	3.5	3.1	0.8
	5+6	3.2	4.6	4.1	2.7	5+7	2.1	3.5	3.0	4.2
	7+8	4.9	6.4	5.8	1.6	6+8	2.9	4.6	4.2	0.2
D	1+2	2.9	4.3	3.9	1.8	1+3	2.1	3.6	3.0	0.2
	3+4	1.9	3.3	2.8	3.5	2+4	1.7	3.4	3.1	1.5
	5+6	3.3	4.8	4.3	0.9	5+7	2.6	4.0	3.4	3.7
	7+8	4.1	5.7	5.3	3.9	6+8	3.2	4.6	4.1	1.2

M=2). When M=1, the equations of Section III(c) reduce to the non-diversity Nakagami statistics for arbitrary m and Ω. Maximum likelihood estimated m parameters for SC, MRC and EGC were greatest for vertical separations in the anechoic chamber. Median m values calculated over the entire set of measurements incorporating transmitter positions A to D are shown in Table III.

For vertically separated antennas in the open office area, the m parameter, although lower than those estimated for the anechoic chamber (presumably due to the additional multipath generated by the surrounding environment), was still relatively large. Nakagami-m values $\gg 1$ in both of these environments suggesting low levels of scattering. The statistics for horizontal combinations were similar to those obtained for vertical combiners. For all horizontal combiners (not shown in Table III) in the open office area the Nakagami-Ω parameter, was found to be (median, max/min): SC (0.84, 0.90/0.78), MRC (0.51, 0.54/0.50) and EGC (0.52, 0.58/0.50), with vertical combiners exhibiting similar performance.

2) User Mobile: Here, the m parameters were reduced compared to stationary measurements showing that the combined received signal envelope is composed of an increased number of fades. Linear correlation between transmitter location and horizontal m-value in the anechoic chamber was found to be SC (0.36), MRC (0.36) and EGC (0.34), suggesting a moderate association between degree of scattering and transmitter location. For vertically separated receivers in both arrays correlation between transmitter location and degree of scattering was much lower, with a maximum of 0.10 for SC. Table IV shows the ML estimated diversity statistics for each of the combining techniques in the open office area. These channels experienced the greatest amount of fading over all those analyzed with both arrays being particularly affected when the transmitter was at positions C and D. Pearson's product moment (Table III) highlights the relationship between transmitter position and the amount of fading observed in the diversity receiver. Fig.6 shows the empirical and theoretical cdfs for the earlier example of branches 7+8 of array 2 (transmitter at C). The symbols in Figs. 6-8 correspond to the theoretical diversity combining plots while the solid lines are the respective empirical plots. It is clear that all three theoretical distributions provide a good description of the empirical distribution functions with minor discrepancies occurring for probabilities less than 0.001.

The LCR and AFD of a signal envelope provides useful information when selecting transmission bit rates, word lengths and coding schemes in digital radio systems and allows an assessment of system performance [22]. Fig.7 presents the empirical and theoretical LCRs, normalized to the maximum Doppler frequency, for branches 7+8 of array 2 (transmitter at C, user mobile, open office area). All crossing rates and fade durations were calculated in the range -20 to 10 dB in steps of 0.5 dB. For this set of combiners, where predicted m parameters tended towards unity, all three combining schemes offered similar fading performance. This is also evident from the AFD plots where all three schemes experienced normalized AFDs of 0.3 at signal levels 10 dB below the local mean. If identical Nakagami fading conditions are assumed for each branch, the individual pre-detection envelopes which made up the diversity system of branches 7+8 will have ML estimated distribution parameters (denoted by subscript combiner) m_{SC}=1.23, Ω_{SC}=0.76, m_{MRC}=1.15, Ω_{MRC}=0.56 and m_{EGC}=1.11, Ω_{EGC}=0.62 (Table IV).

A simulated diversity envelope was produced using the Nakagami waveform generator described in [18], which was programmed with the individual ML estimated Nakagami distribution parameters to generate the signal envelopes as seen by each antenna of the dual branch on-body diversity receiver for each type of combiner. These were then combined using equations (2) to (4). Fig.9 shows the simulated SC, MRC and EGC AFDs alongside the empirical data.

V. DISCUSSION OF ON-BODY DIVERSITY RESULTS

Consider horizontal dual branch diversity for a stationary user in the anechoic chamber with the transmitter at position A at the front of the body. Here, both antenna elements are excited by the same dominant component, thus mean signal levels are expected to be comparable meaning that diversity may be helpful. As the transmitter is positioned at points A to D the creeping wave contribution, which is the main propagation mode around the surface of the body [23], may arrive

TABLE III
SUMMARY STATISTICS FOR NAKAGAMI-m PARAMETERS OVER ALL SCENARIOS

	Horizontal								
	SC			MRC			EGC		
Scenario	Med.	Max	Min	Med.	Max	Min	Med.	Max	Min
AC / Stat.	8.01	18.5	3.86	8.54	27.7	4.46	8.60	33.5	4.63
AC / Mob.	3.27	5.36	1.34	3.23	4.28	1.15	3.27	4.29	1.18
OO / Stat.	6.22	20.3	1.88	5.95	27.3	1.71	5.96	45.3	1.75
OO / Mob.	1.75	4.68	0.72	1.69	4.52	0.70	1.69	4.62	0.70
Vertical									
AC / Stat.	9.75	17.0	2.51	9.68	29.6	2.29	9.48	43.1	2.33
AC / Mob.	2.81	7.94	1.42	2.63	6.47	1.33	2.64	6.33	1.36
OO / Stat.	6.04	14.3	1.43	5.55	16.7	1.38	5.62	16.0	1.43
OO / Mob.	1.55	4.18	0.63	1.42	3.73	0.55	1.42	3.79	0.54

TABLE IV
ML ESTIMATED NAKAGAMI DIVERSITY PARAMETERS FOR DUAL BRANCH SC, MRC AND EGC WHILE USER WAS MOBILE IN THE OPEN OFFICE AREA

TX Position	Horizontal							Vertical						
	SC			MRC		EGC		SC			MRC		EGC	
	Branch	m	Ω	m	Ω	m	Ω	Branch	m	Ω	m	Ω	m	Ω
A	1+2	3.02	0.80	2.57	0.53	2.59	0.55	1+3	4.18	0.82	3.73	0.52	3.79	0.53
	3+4	4.68	0.82	4.52	0.51	4.62	0.53	2+4	2.81	0.80	2.59	0.53	2.63	0.55
	5+6	2.26	0.79	2.16	0.53	2.21	0.56	5+7	2.89	0.80	2.75	0.52	2.74	0.55
	7+8	3.43	0.81	3.25	0.52	3.22	0.54	6+8	2.46	0.79	2.19	0.53	2.21	0.56
B	1+2	2.72	0.79	2.83	0.52	2.93	0.54	1+3	1.98	0.78	2.14	0.53	2.24	0.56
	3+4	2.02	0.78	2.09	0.53	2.15	0.56	2+4	2.88	0.80	2.83	0.52	2.88	0.54
	5+6	2.52	0.79	2.56	0.52	2.62	0.55	5+7	2.11	0.78	1.86	0.54	1.89	0.57
	7+8	2.93	0.80	2.71	0.52	2.71	0.55	6+8	2.76	0.79	2.68	0.52	2.71	0.55
C	1+2	0.85	0.76	0.81	0.58	0.80	0.67	1+3	0.84	0.77	0.82	0.58	0.83	0.67
	3+4	1.02	0.77	0.96	0.57	0.96	0.65	2+4	0.76	0.77	0.69	0.60	0.69	0.70
	5+6	0.94	0.76	0.91	0.58	0.90	0.66	5+7	0.88	0.76	0.81	0.58	0.79	0.67
	7+8	1.23	0.76	1.15	0.56	1.11	0.62	6+8	0.78	0.77	0.73	0.6	0.73	0.69
D	1+2	1.04	0.76	0.94	0.57	0.93	0.65	1+3	1.12	0.76	0.97	0.56	0.95	0.64
	3+4	1.48	0.77	1.29	0.55	1.23	0.61	2+4	1.02	0.76	0.93	0.57	0.92	0.65
	5+6	0.72	0.77	0.7	0.6	0.7	0.7	5+7	0.63	0.78	0.55	0.63	0.54	0.77
	7+8	0.77	0.77	0.72	0.6	0.72	0.7	6+8	0.77	0.77	0.7	0.61	0.69	0.71
Correlation		-0.73		-0.74		-0.75			-0.78		-0.81		-0.81	

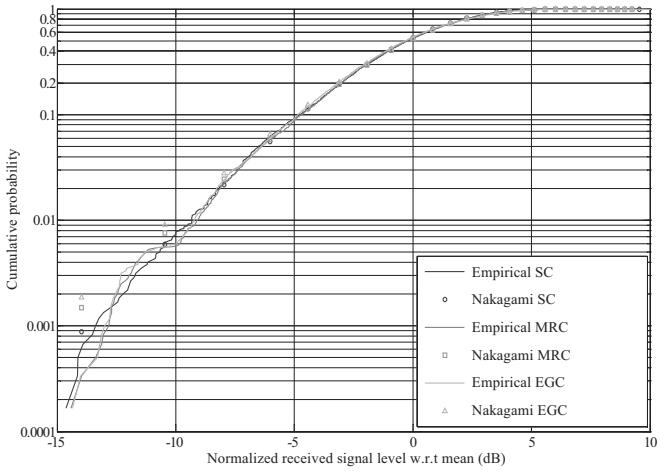

Fig. 6. Empirical (solid line) and theoretical Nakagami (symbols) cumulative distribution plots for on-body diversity combining using branches 7+8 while the user was mobile in the open office area with transmitter at C. Theoretical plots have Nakagami parameters: SC, $m = 1.23$ and $\Omega = 0.76$; MRC, $m = 1.15$ and $\Omega = 0.56$; EGC, $m = 1.11$ and $\Omega = 0.62$.

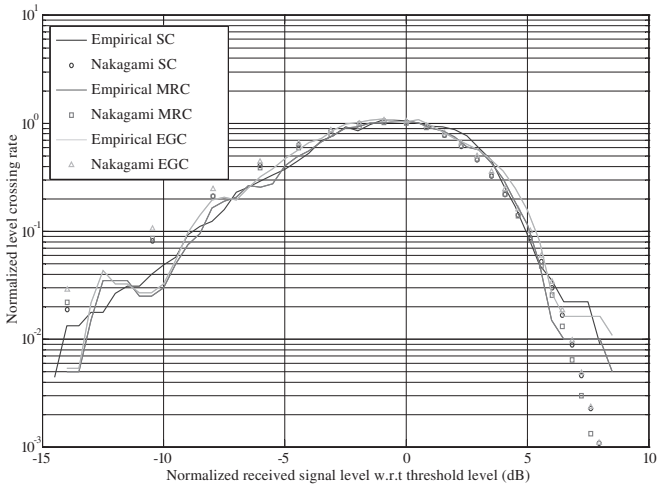

Fig. 7. Normalized level crossing rates for each of the three combining techniques using horizontally separated branches 7+8 of the on-body diversity system while the user was mobile in the open office area with transmitter at position C. Theoretical Nakagami parameters are given in Table IV.

from more than one direction, hence the signal will appear attenuated possibly beyond the mean level of the other branch rendering diversity less effective. Furthermore, for the user stationary in the open office area, multipath from the building surroundings does not make any major contribution as the body surface remains the primary mechanism for propagation (supported by high m parameters - median > 5.55). However, when the user is mobile, the surface wave contribution may become attenuated and periodically interrupted due to limb movements, particularly for the longer paths (back positions C and D) leading to reduced m parameters and slightly increased diversity gain. When movement is combined with

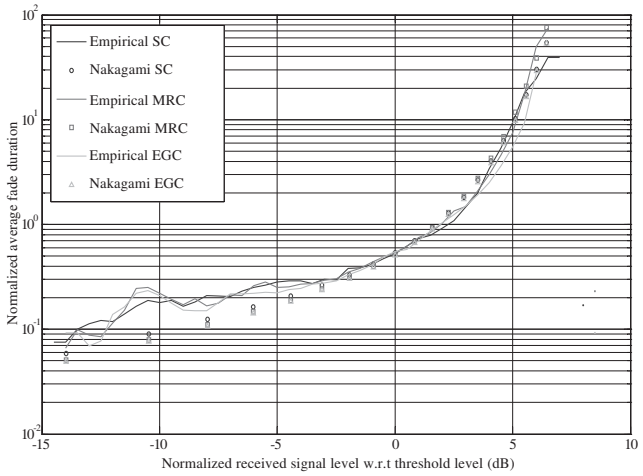

Fig. 8. Normalized average fade durations for each of the three combining techniques using horizontally separated branches 7+8 of the on-body diversity system while the user was mobile in the open office area with transmitter at position C. Theoretical Nakagami parameters are given in Table IV.

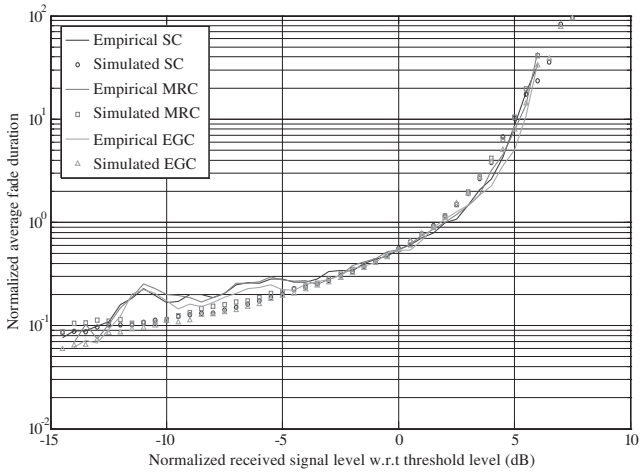

Fig. 9. Empirical (solid line) and simulated (symbols) average fade durations for each of the three combining techniques using horizontally separated branches 7+8 of the on-body diversity system while the user was mobile in the open office area with transmitter at position C.

the increased multipath contribution, scattering and reflection from nearby objects / structures of the open office area, the net result may be to further increase diversity gain. This view is supported by the ML estimated m parameters for combined branch envelopes (Table IV) at transmitter locations C and D, where $m \rightarrow 1$ (combiners operating in Rayleigh fading, i.e., no dominant component). These channel conditions mean that signal levels are comparable and with a branch correlation of less than 0.7 the prospects for the useful implementation of receiver diversity are extremely good.

For stationary vertical separations in both anechoic and open office area environments, no clear pattern between transmitter location and diversity gain / channel statistics was evident. However, when the user was mobile in the open office area the same dependency upon receiver position as obtained for horizontal combiners was apparent, reinforcing the fact that all signal contributions for channels which cross front to back body in highly multipath environments are composed of scattered contribution from the body and local surroundings.

VI. Conclusion

In this paper we have examined the performance of three common diversity combination schemes for use in two-branch spatial on-body diversity systems. A comparison of cross-correlation and diversity gain (at 90% signal reliability) was made based upon on-body transmitter - receive array separation, user activity and type of environment. The results have shown that, despite the compact spacing between array elements, CCCs are typically less than 0.7. Diversity gain was found to be highest when the user was mobile in the open office area, in particular for the cases where the main propagation path traverses from one side of the user's body to the other (non-line of sight). Conversely, when the user was stationary, diversity gain decreased for all three combining schemes. The selection combination scheme performed worst overall with median diversity gain always below 0.3 dB, with the exception of mobile measurements in the open office area (1.4 dB). For MRC and EGC, diversity gain was always greater than 2.0 dB. These results lead to the conclusion that sufficient benefits from implementing on-body spatial diversity may only be realized for cases where on-body links cross from one side of the body to the other and the user is expected to be mobile in a multipath environment. Furthermore, in this paper a novel statistical characterization of the fading experienced in on-body diversity channels was performed using purposely derived first and second order diversity combining statistics. We also provide a selection of ML estimated m and Ω parameters for various SC, MRC and EGC dual branch combiners operating in Nakagami fading so that our results may be reproduced.

References

[1] H. R. Chuang, "Human operator coupling effects on radiation characteristics of a portable communication dipole antenna," *IEEE Trans. Antennas Propag.*, vol. 42, pp. 556–560, Apr. 1994.

[2] W. G. Scanlon and N. E. Evans, "Numerical analysis of bodyworn UHF antenna systems," *IEE Electronics & Comms. Eng. J.*, vol. 13, no. 2, pp. 53–64, Apr. 2001.

[3] A. Molisch, *Wireless Communications*. IEEE Press/Wiley, 2005.

[4] S. L. Cotton and W. G. Scanlon, "A statistical analysis of indoor multipath fading for a narrowband wireless body area network," *17th IEEE Intl. Symp. Personal, Indoor & Mobile Radio Comms. (PIMRC)*, pp. 1–5, Helsinki, Finland, Sept. 2006.

[5] S. L. Cotton and W. G. Scanlon, "Characterization and modeling of the indoor radio channel at 868 MHz for a mobile bodyworn wireless personal area network," *IEEE Antennas Wireless Propag. Lett.*, vol. 6, pp. 51–55, 2007.

[6] A. Fort, C. Desset, P. De Doncker, P. Wambacq, and L. Van Biesen, "An ultra-wideband body area propagation channel Model-from statistics to implementation," *IEEE Trans. Microw. Theory Tech.*, vol. 54, pp. 1820–1826, June 2006.

[7] A. Fort, J. Ryckaert, C. Desset, P. De Doncker, P. Wambacq, and L. Van Biesen, "Ultra-wideband channel model for communication around the human body," *IEEE J. Select. Areas Commun.*, vol. 24, pp. 927–933, Apr. 2006.

[8] M. Nakagami, "The m-distribution: a general formula of intensity distribution of rapid fading," in *Statistical Methods in Radio Wave Propagation*. New York: Pergamon, pp. 3–36, 1960.

[9] N. C. Beaulieu and A. A. Abu-Dayya, "Analysis of equal gain diversity on Nakagami fading channels," *IEEE Trans. Commun.*, vol. 39, pp. 225–234, Feb. 1991.

[10] E. Al-Hussaini and A. Al-Bassiouni, "Performance of MRC diversity systems for the detection of signals with Nakagami fading," *IEEE Trans. Commun.*, vol. 33, pp. 1315–1319, Dec.1985.

[11] P. R. Sahu and A. K. Chaturvedi, "Performance analysis of predetection EGC in exponentially correlated Nakagami-m fading channel," *IEEE Trans. Commun.*, vol. 53, pp. 1252–1256, Aug. 2005.

[12] O. C. Ugweje, "Selection diversity for wireless communications in Nakagami-fading with arbitrary parameters," *IEEE Trans. Veh. Technol.*, vol. 50, pp. 1437–1448, Nov. 2001.
[13] S. O. Rice, "Statistical properties of a sine wave plus random noise," *Bell Syst. Tech. J.*, vol. 27, pp. 109–157, Jan. 1948.
[14] M. D. Yacoub, C. R. C. M. da Silva and J. E. Vargas Bautista, "Second-order statistics for diversity-combining techniques in Nakagami-fading channels," *IEEE Trans. Veh. Technol.*, vol. 50, pp. 1464–1470, Nov. 2001.
[15] C. D. Iskander and P. Takis Mathiopoulos, "Analytical level crossing rates and average fade durations for diversity techniques in Nakagami fading channels," *IEEE Trans. Commun.*, vol. 50, pp. 1301–1309, Aug. 2002.
[16] IEEE Standards for Information Technology Part 15.4: Wireless Medium Access Control (MAC) and Physical Layer (PHY) Specifications for Low-Rate Wireless Personal Area Networks (LR-WPANs), IEEE Std. 802.15.4-2003, 2003.
[17] U. Varshney and S. Sneha, "Patient monitoring using adhoc wireless networks: Reliability and power management," *IEEE Commun. Mag.*, vol. 44, pp. 49–55, Apr. 2006.
[18] J. C. S. S. Filho, M. D. Yacoub, and G. Fraidenraich, "A simple accurate method for generating autocorrelated Nakagami-m envelope sequences," *IEEE Commun. Lett.*, vol. 11, pp. 231–233, Mar. 2007.
[19] W. C. Jakes, *Microwave Mobile Communications*. New York: Wiley, 1974.
[20] K. Dietze, C. B. Dietrich Jr., and W. L. Stutzman, "Analysis of a two-branch maximal ratio and selection diversity system with unequal SNRs and correlated inputs for a Rayleigh fading channel," *IEEE Trans. Wireless Commun.*, vol. 1, pp. 274–281, Apr. 2002.
[21] A. M. D. Turkmani, A. A. Arowojolu, P. A. Jefford, and C. J. Kellett, "An experimental evaluation of the performance of two-branch space and polarization diversity schemes at 1800 MHz," *IEEE Trans. Veh. Technol.*, vol. 44, pp. 318–326, May 1995.
[22] J. D. Parsons, *The Mobile Radio Propagation Channel*, 2nd ed. John Wiley & Sons. 2000.
[23] J. Ryckaert, P. Doncker, R. Meys, A. de Le Hoye, and S. Donnay, "Channel model for wireless communication around human body," *Electron. Lett.*, vol. 40, no. 9, pp. 543–544, Apr. 2004.

Simon L. Cotton (S'04-M'07) received the B.Eng. degree in electronics and software from the University of Ulster, UK in 2004 and the Ph.D. degree in electrical and electronic engineering from the Queen's University of Belfast, Belfast, UK in 2007. He is currently working as a Research Fellow with the Radio Communications Research Group of the Institute of Electronics, Communications and Information Technology (ECIT), Belfast, UK, where he is investigating millimeter-wave technologies for personal communications and novel applications of short-range radio systems. His research interests include radio channel characterization and modeling for wireless body and personal area networks, measurements for transceiver diversity in bodyworn applications and simulation of wireless channels. Dr. Cotton has authored and co-authored over 20 publications in major IEEE/IET journals and refereed international conferences.

William G. Scanlon (M'97) (M'98) received the B.Eng. degree in electrical engineering (first-class honours) by part-time study and the Ph.D. degree in electronics (specializing in wearable and implanted antennas) from the University of Ulster, UK in 1994 and 1997, respectively. He was appointed as Lecturer at the University of Ulster in 1998, then Senior Lecturer and Full Professor at Queen's University of Belfast (UK) in 2002 and 2008, respectively. He currently leads the Radio Communications research group at Queen's. Prior to starting his academic career he had 10 years of industrial experience, having worked as a Senior RF Engineer for Nortel Networks, as a Project Engineer with Siemens and as a Lighting Engineer with GEC-Osram. Prof. Scanlon's current research interests include personal communications, wearable antennas, RF and microwave propagation, channel modeling and characterization, wireless networking and protocols and wireless networked control systems. He has published over 140 research papers in major IEEE/IET journals and in refereed international conferences. He served as a keynote speaker for the European Workshop on Conformal Antennas (2007). He will Co-Chair the 2009 Loughborough Antennas and Propagation Conference and he has acted as invited speaker and session chair at numerous other national and international conferences. Prof. Scanlon received a Young Scientist award from URSI in 1999, he is a prolific reviewer for IEEE/IET journals and conferences and other major conferences. He is a member of the IEEE International Committee on Electromagnetic Safety (ICES) and the IASTED International Committee on Telecommunications.